J. Vis. Commun. Image R. 26 (2015) 296–304

Contents lists available at ScienceDirect

J. Vis. Commun. Image R.

journal homepage: www.elsevier.com/locate/jvci

Random-valued impulse noise removal using adaptive dual threshold median filter

Vikas Gupta *, Vijayshri Chaurasia, Madhu Shandilya

Maulana Azad National Institute of Technology, Bhopal, MP, India

ARTICLE INFO

Article history:
Received 17 March 2014
Accepted 1 October 2014
Available online 17 October 2014

Keywords:
Image de-noising
Median filter
Noise detection
Noise removal
Random-valued impulse noise
Dual threshold
Two-stage scheme
Filtering window

ABSTRACT

Noise detection and its removal is very important in the image processing. Detection of noise is very crucial and significant in random valued impulse noise because it does not hamper the image pixels uniformly. This paper presents a novel and unique concept of adaptive dual threshold for the detection of random valued impulse noise along with simple median filter at noise removal stage. Simulation results shows that an efficient noise detection leads to a superior quality of de-noised image as compared to existing adaptive threshold based image de-noising techniques. Proposed threshold computation is based on averaging of pixel values of window which enhances the PSNR of our system as compared to existing median filter based image de-noising methods.

© 2014 Elsevier Inc. All rights reserved.

1. Introduction

Image de-noising is an essential pre-processing step for image analysis. It refers to the process of recovering a good estimate of the original image from a corrupted one, without altering and changing useful information in the image such as discontinuities and edges [1,18]. During the acquisition or transmission of images, they are frequently corrupted by noise and this degrades the quality of an image along with other features like sharpness, edge, layer depth, etc. Hence noise detection and its removal is very important image processing task for many applications. Noise is generally modelled as Gaussian noise (Normal), Uniform noise and Impulse noise. Impulse noise is randomly distributed over the image and is of two types: Fixed Value Impulse Noise (FVIN) and Random Valued Impulse Noise (RVIN) [3]. Removal of RVIN is more important and complex since it corrupts the pixels with any magnitude in the available gray level [4].

Many algorithms have been proposed to remove the effect of RVIN [5–15], but most of them cause the blurring of edges in the image [2]. In image de-noising the noisy pixels are first detected and then gray levels of noisy pixels are modified by a locally computed approximate value [1]. Detection stage identifies the noisy and noise free pixels of the corrupted image. Proposed method utilizes windowing technique in noise detection stage. In this process, first of all, a test window is defined and central pixel of the window is checked with respect to some defined threshold for identifying the existence of noise. And after the detection of noisy pixel, noise removal part eradicates the noise from it. Quality of noise detection is very much dependent on the selection of threshold value. Most of the techniques compute a priori threshold for all the filtering windows depending on image details while some of the techniques also work in an adaptive manner where threshold value for each window is computed separately.

Filters are simple and efficient solution for the removal of noise, they fall in two categories: linear filter and non-linear filter [5]. Linear filters are low pass filters and tend to blur the edges and other details of image. On the other hand, non-linear filters remove the impulse noise without edge blurring and results in better image quality thereby causing more complexity in the system. Median filter [1] is a widely used non-linear filter in image de-noising due to its effectiveness and high computational efficiency. This conventional method modifies all the pixels of image by median of its surrounding pixels, irrespective of the existence/absence of noise. It leads to the loss of fine image details causing an edge jitter and streaking. At high noise densities simple median filter also results in some patches [2].

Lots of improvement in simple median filter has been proposed to make a trade-off between detail preservation and complexity. Most of them are the Tri-State Median Filter (TSMF) [7], the Multi-state Median Filter [8], the Centre Weighted Median Filter (CWMF)

* Corresponding author.
E-mail addresses: vgup24@yahoo.com (V. Gupta), vijayshree21@gmail.com (V. Chaurasia), madhu_shandilya@yahoo.in (M. Shandilya).

http://dx.doi.org/10.1016/j.jvcir.2014.10.004
1047-3203/© 2014 Elsevier Inc. All rights reserved.

[9], the Rank-Order Mean Filter [10] and the Stack Filter [11]. However these filters are applied uniformly over the whole image, without considering whether the test pixel is a noisy pixel or not [6]. This might modify the image details and cause image quality degradation. In order to overcome this shortcoming, the switching scheme or the two-stage method has been introduced. The Basic Principle in this two stage scheme is that noisy pixels are detected first and filtered afterward, whereas uncorrupted pixels are left unchanged. Notable de-noising method based on this two-stage scheme are: Progressive Switching Median Filter (PSMF) [12], Luo-Iterative Median Filter (Luo) [13], Adaptive Switching Median Filter (ASMF) [14] and Adaptive Non-Local Switching Median Filter (ANSM) [15], etc. The performance may further improve by incorporating the sorting algorithm with median filter to sort the elements of window [16]. Recently some probabilistic methods are also investigated for image noise removal, like in de-noising of astronomical images (SAR images) [20–22] and layer depth de-noising [19], etc.

In the proposed method, we have improved the technique of noise detection by introducing the concept of two threshold values for detection of RVIN. It results in efficient detection and provides better quality of de-noised image. Dual threshold concept is already investigated by K.S. Srinivasan and D. Ebnezer in 2007 for the detection of FVIN [17]. Threshold computation of Srinivasan's method was based on the rearrangement of pixels in the window. In our method, thresholds are estimated by averaging process and provide brilliant quality of recovered image by using Simple Median [MED] filter for noise removal.

Rest of the paper is organized as follows: In Section 2, noise model for random valued impulse noise is discussed. Section 3 presents the important features of different median filter based de-noising methods. Section 4 furnishes proposed de-noising method. In Section 5, simulation results of proposed method on test images are given. Finally, a brief conclusion is presented in Section 6.

2. Impulse noise model

In Random valued impulse noise (RVIN), noise is dispersed uniformly. RVIN may take any value in the dynamic range of [0, 255]. At any pixel location (i,j), let $Y_{i,j}$ be the gray level of original image Y and $X_{i,j}$ be the gray level of noisy image and $[n_{min}, n_{max}]$ be the dynamic range of image gray levels. For 8-bit images, $n_{min} = 0$ and $n_{max} = 255$. An image contaminated by RVIN with probability p can be described as follow:

$$X_{ij} = \begin{cases} n_{ij} & \text{with probability} \quad p \\ Y_{ij} & \text{with probability} \quad 1-p \end{cases} \tag{1}$$

where n_{ij} denotes the uniformly distributed random number in $[n_{min}, n_{max}]$, that is n_{ij} can be any number between n_{min} and n_{max} [15]

3. Median filter based de-noising methods

Median filter is one of the most important non-linear filters which are used to remove RVIN. In this filter, the value of corrupted pixel in noisy image is replaced by the median value of the corresponding window. Median value is the value in the middle position of any sorted sequence [1].

Consider that the gray levels of any pixel value, in any window (w_x) of size $n \times n$ are represented by $x_1, x_2, x_3, \cdots, x_n$ and it becomes $x_{i1} \geqslant x_{i2} \geqslant x_{i3} \ldots \geqslant x_{in}$ after sorting it in descending or in an ascending order

$$M_x = \text{Median}(w_x) = \begin{cases} x_{i(n+1)/2}; & n \text{ is odd} \\ \frac{1}{2}\left[x_{i\left(\frac{n}{2}\right)} + x_{i\left(\frac{n}{2}\right)+1}\right]; & n \text{ is even} \end{cases} \tag{2}$$

Various median filter based image de-noising methods have been proposed in literature, many of them are application oriented. Some of the significant methods have been explained below.

3.1. Switching median filter (SWM)

A switching median (SWM) filter is a two steps scheme. In the first step, each pixel is checked whether it is a noisy or not. A pixel is said to be contaminated by noise if the absolute difference between the median value in its neighborhood and the value of the current pixel itself is greater than a given threshold. If the said condition is satisfied, a simple median filter is applied in the second phase, if not then the current pixel is said to be noise free and will remain unchanged. Consider an image X corrupted by an impulse noise and $X_{i,j}$ be the gray level value of the noisy image at position (i, j). Let W be the square window covering this pixel of size $(2L + 1) \times (2L + 1)$, where L is an integer greater than zero. The output $Z_{i,j}$ of switching median filter is given by

$$Z_{i,j} = \begin{cases} m_{i,j}, & if\,|m_{i,j} - X_{i,j}| > \text{Threshold} \\ X_{i,j}, & \text{otherwise} \end{cases} \tag{3}$$

where $m_{i,j}$ is the median value in the window W and Threshold is a fixed parameter [14]. Here the value of threshold is either defined a priori or selected after many data dependant tests.

3.2. Adaptive Switching Median Filter (ASWM)

The Adaptive Switching Median Filter is an improvised version of SWM filter. Here Threshold is not a priori choice but computed locally from image pixels. Now in every filtering window, weighted means are iteratively estimated. Then the weighted standard deviation is calculated and Threshold is determined. This filter provides improved results since impulse noise does not corrupt the statistics

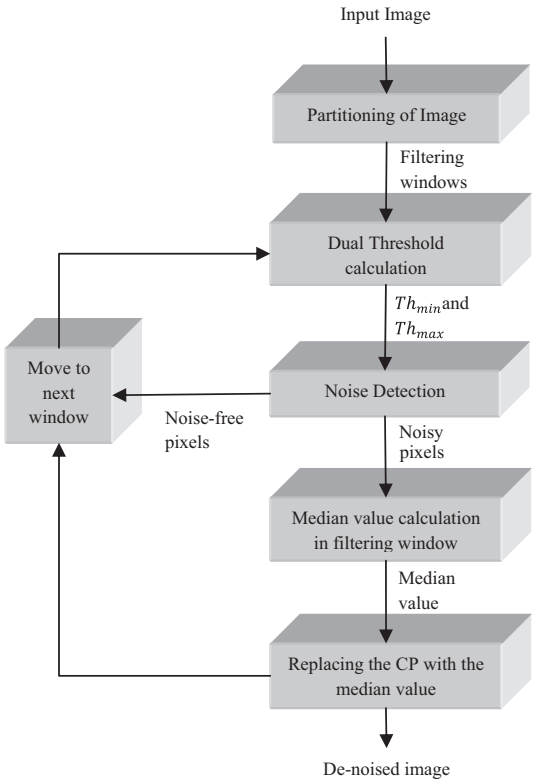

Fig. 1. Block diagram representation of proposed image de-noising method.

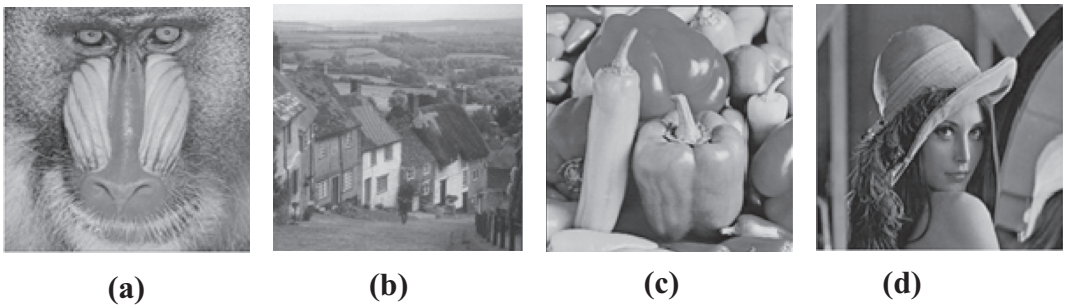

Fig. 2. Original JPEG grayscale test images of 8-bit per pixel. (a) Mandrill. (b) Gold-hill. (c) Pepper and (d) Lena.

Table 1
PSNR (dB) values of different filters for Mandrill image corrupted by RVIN.

Method	10%	20%	30%	40%	50%	60%	70%
MED [1]	28.81	27.43	25.49	23.62	22.59	21.50	19.80
TSM [7]	32.36	29.22	26.08	24.27	23.48	21.20	20.01
PSMF [12]	29.01	26.55	24.93	23.73	22.61	21.60	20.81
CWMF [9]	30.91	28.05	24.99	23.97	22.75	21.8	20.42
Luo [13]	32.69	29.74	26.83	24.92	22.06	21.32	19.95
ASWM [14]	33.15	30.18	27.91	26.70	24.60	22.51	21.22
ANSM [15]	32.71	30.08	28.30	26.78	24.42	23.01	21.82
Proposed	35.93	34.39	32.77	31.59	29.87	28.69	26.51

Table 2
PSNR (dB) values of different filters for Gold-hill image corrupted by RVIN.

Method	10%	20%	30%	40%	50%	60%	70%
MED [1]	27.93	26.21	25.58	24.87	24.03	23.30	22.28
TSMF [7]	34.23	30.74	29.30	27.40	25.42	24.01	22.87
PSMF [12]	29.73	27.17	25.99	25.33	24.56	22.52	21.64
CWMF [9]	32.55	30.01	28.58	26.98	25.08	24.62	23.5
Luo [13]	33.44	31.31	28.61	25.47	23.01	21.02	20.05
ASWM [14]	35.99	33.01	30.57	29.51	26.73	24.58	22.01
ANSM [15]	35.38	32.88	30.76	29.46	26.43	24.62	21.80
Proposed	36.91	35.38	33.25	31.78	29.84	28.22	26.74

Table 3
PSNR (dB) values of different filters for Pepper image corrupted by RVIN.

Method	10%	20%	30%	40%	50%	60%	70%
MED [1]	30.05	28.32	26.82	25.38	23.97	21.01	20.02
TSMF [7]	32.05	31.34	27.62	23.17	20.20	18.85	17.52
PSMF [12]	34.05	32.99	30.05	28.90	25.52	23.12	21.52
CWMF [9]	32.55	30.00	28.58	26.98	25.08	23.52	21.61
Luo [13]	35.89	34.39	31.50	28.90	24.89	23.12	20.85
ASWM [14]	36.02	34.55	32.65	31.03	27.61	25.96	22.62
ANSM [15]	36.51	34.73	32.52	31.47	28.42	26.88	23.71
Proposed	40.68	37.83	35.03	32.13	30.02	28.37	26.79

Table 4
PSNR (dB) values of different filters for Lena image corrupted by RVIN.

Method	10%	20%	30%	40%	50%	60%	70%
MED [1]	30.46	28.85	27.16	25.65	24.30	22.91	21.21
TSMF [7]	36.87	32.37	30.50	28.48	25.39	23.52	20.10
PSMF [12]	34.21	32.78	30.34	28.07	26.70	24.28	21.61
CWMF [9]	35.02	31.64	29.67	28.12	25.06	23.61	21.52
Luo [13]	36.11	34.77	30.42	29.62	25.80	24.01	22.51
ASWM [14]	36.51	34.33	32.49	31.04	28.02	26.75	24.52
ANSM [15]	36.62	35.31	33.09	31.25	28.96	**27.31**	24.61
Proposed	41.02	38.09	34.67	31.45	29.15	27.02	24.78

Bold value defines the superiority of our proposed method in terms of PSNR as compared to other already existing de-noising methods.

of image. Consider an image X corrupted by an impulse noise and X_{ij} be the gray level value of the noisy image at pixel location (i, j). The restored image Z_{ij} by ASWM filter is given by

$$Z_{ij} = \begin{cases} m_{ij}, & if\,|X_{ij} - M_{ij}| > \alpha \times \delta_{ij} \\ X_{ij}, & \text{otherwise} \end{cases} \quad (4)$$

where M_{ij}, δ_{ij} and m_{ij} are the weighted mean, weighted standard deviation and the median respectively. || denotes the absolute value operator, $\alpha \times \delta_{ij}$ is the local threshold. Here "α", is a given parameter whose value is decremented with fixed and defined value in

Table 5
Average PSNR (dB) performance of different filters considering four test images of Fig. 2, corrupted by RVIN.

Method	10%	20%	30%	40%	50%	60%	70%
MED [1]	29.31	27.70	26.26	24.88	23.72	22.18	20.83
TSMF [7]	33.87	30.92	28.37	25.83	23.62	21.89	20.12
PSMF [12]	31.75	29.87	27.96	26.51	24.85	22.88	21.39
CWMF [9]	32.75	29.92	29.34	26.51	24.49	23.39	21.76
Luo [13]	34.53	32.55	29.34	27.23	23.94	22.37	20.84
ASWM [14]	35.41	33.01	30.91	29.57	26.74	24.95	22.59
ANSM [15]	35.30	33.25	31.17	29.74	27.06	25.46	22.99
Proposed	38.63	36.42	33.93	31.74	29.72	28.08	26.21

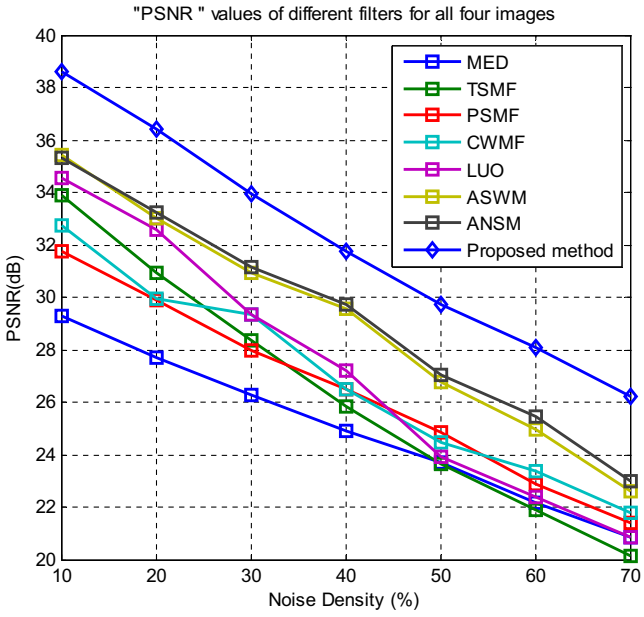

Fig. 3. Comparative chart of average PSNR performance of different filters given in Table 5.

every iteration. Adaptability of this method is the important factor to preserve image details [14].

3.3. Adaptive Non-Local Switching Median Filter (ANSM)

In this filter, a better noise detector is used to detect the noise candidate at high noise densities. In this, first of all, a test window of size 3×3 is chosen and thereafter the processing pixel $X_{i,j}$ is checked for the existence of noise. Each processing pixel would exist in nine sub-windows of size 3×3 and for each such sub-window a weighted mean $M_{k,i,j}$ and a weighted standard deviation $\delta_{k,i,j}$ is calculated. Now the processing pixel at location (i,j) is checked for noise

$$(i,j) = \begin{cases} \text{noisy pixel}, & \text{if } \text{sum}|X_{i,j} - M_{k,i,j}| > \alpha \times \delta_{k,i,j} > n \\ \text{noise-free pixel}, & \text{otherwise} \end{cases} \tag{5}$$

where $X_{i,j}$ and n are the gray level of noisy pixel at pixel location (i,j) and a Threshold respectively. Here also || denotes the absolute value operator and *sum* represents the total of the nine sub-windows in which the condition is satisfied i.e. the absolute difference is greater than the corresponding local threshold $\alpha \times \delta_{k,i,j}$ for $k \in [1, 2, \cdots 9]$. In other words, if the total number is greater than the threshold n, the processing pixel is considered as noisy otherwise it is well concluded as noise free [15].

4. Proposed method

The proposed de-noising method is a median filter based technique with adaptive dual threshold. In single threshold system, when central pixel is checked for the presence of noise, any pixel value lesser than (or greater than) the given single threshold will be considered as noise. In this system, the range of pixel values used for identifying the noisy pixels will be large. This may increase the possibility of incorrect detection. In the proposed adaptive dual threshold system, the noisy pixels are identified in a relatively narrow range and thus can reduce the probability of incorrect detection. In the proposed method, the image to be de-noised is partitioned into sub-images (filtering windows). For any given $N \times N$ gray level image which is defined by $f{:}N \times N \to I$, where $I = [a, b]$ represents the range of pixel values. Pixel value at location (i,j) is given by $f(i,j)$. Let $r \times r$ be the size of filtering window "W", formed by partitioning of image. Now, the existence of noise is identified at the central pixel (CP) of distinct filtering window with respect to certain defined thresholds. Proposed dual threshold based noise detection and removal process is represented in the block diagram shown in Fig. 1.

A generalized filtering window "W", is given in Eq. (6), it has r rows and r columns. The gray level at any pixel (i,j) is represented by $X_{(i,j)}$:

$$w = \begin{bmatrix} X_{(1,1)} & \cdots & X_{\left(1,\frac{r+1}{2}\right)} & \cdots & X_{(1,r)} \\ \vdots & \ddots & \vdots & & \vdots \\ X_{\left(\frac{r+1}{2},1\right)} & \cdots & X_{\left(\frac{r+1}{2},\frac{r+1}{2}\right)} & \cdots & X_{\left(\frac{r+1}{2},r\right)} \\ \vdots & & \vdots & \ddots & \vdots \\ X_{(r,1)} & \cdots & X_{\left(r,\frac{r+1}{2}\right)} & \cdots & X_{(r,r)} \end{bmatrix} \tag{6}$$

In images, gradual changes in adjacent pixel values are more common as compared to the abrupt changes. Noise corruption at any pixel would change its gray level with respect to its surrounding pixels. Average values of a set of samples (data values) always lie in close proximity to the values under consideration. Hence any sudden change in pixel value can be easily identified by analyzing it with respect to average values. Based on this fact, averages of rows and columns of filtering window are used for threshold computation in proposed method which leads to efficient noise detection. In every filtering window, minimum threshold (Th_{min}) and maximum threshold (Th_{max}) are estimated which are used to detect the abrupt changes in pixel values.

In order to estimate the thresholds, first of all, the averages of elements in individual rows ($A_v(R)$) of filtering window are calculated.

$$A_v(R_r) = \frac{1}{r}\sum_{j=1}^{r} X(r,j) \tag{7}$$

This process will result "r" average values corresponding to every row. After that the averages of elements in individual columns ($A_v(C)$) of filtering window are calculated.

Table 6
Quality performance (PSNR in dB) of proposed method for images corrupted by RVIN using different size of filtering window.

Filtering window size	10%	20%	30%	40%	50%	60%	70%
Lena							
3×3	**41.02**	**38.09**	**34.67**	**31.45**	29.15	27.02	24.78
5×5	36.68	34.83	33.67	31.67	**30.20**	**28.50**	**27.24**
7×7	33.09	32.10	30.82	29.54	28.30	26.82	25.03
Pepper							
3×3	**40.68**	**37.83**	**35.03**	**32.13**	30.02	28.37	26.79
5×5	37.34	35.25	33.58	32.06	**30.45**	**28.66**	**27.53**
7×7	34.29	32.44	30.99	29.80	28.66	27.53	26.82
Goldhill							
3×3	**36.91**	**35.38**	**33.25**	**31.78**	29.84	28.22	26.74
5×5	34.05	33.44	32.35	31.43	**30.46**	**29.28**	**28.21**
7×7	32.50	31.78	30.92	30.08	29.10	28.08	27.32
Mandrill							
3×3	**35.93**	**34.39**	**32.77**	**31.59**	29.87	28.69	26.51
5×5	32.94	32.50	31.89	31.27	**30.62**	**29.83**	**29.25**
7×7	31.81	31.42	30.89	30.38	29.83	29.26	28.63
Average performance							
3×3	**38.63**	**36.42**	**33.93**	**31.74**	29.72	28.07	26.21
5×5	35.25	34.00	32.87	31.61	**30.43**	**29.07**	**28.06**
7×7	32.92	31.94	30.90	29.95	28.97	27.92	26.95

Bold values defines that the proposed method performs better from 10% to 40% noise density for filtering window size of 3×3. By increasing this noise density further, the performance with 5×5 window size becomes better and improvised.

$$A_v(C_r) = \frac{1}{r}\sum_{i=1}^{r} X(i,r) \tag{8}$$

This process will also result "r" average values corresponding to every column. These "$2r$", distinct average values will be used for finding Th_{min} and Th_{max} using following equations:

$$Th_{min} = min\{A_v(R_1),\ldots A_v(R_r), A_v(C_1),\ldots A_v(C_r)\} \tag{9}$$

$$Th_{max} = max\{A_v(R_1),\ldots A_v(R_r), A_v(C_1),\ldots A_v(C_r)\} \tag{10}$$

Now, the noise corruption at CP of filtering window is checked by comparing it with the Th_{min} and Th_{max}. If the CP value lies between thresholds computed by Eqs. (9) and (10), then it is considered as noise free otherwise noisy.

$$CP = \begin{cases} Th_{min} \leqslant CP \leqslant Th_{max}; & \text{Noisefree} \\ \text{Else;} & \text{Noisy} \end{cases} \tag{11}$$

If the CP is estimated as noisy, then the noise removal is need to be applied at specific CP, otherwise it is kept same and filtering window is shifted to the next pixel. At the noise removal stage, simple median (M) of filtering window have been used to modify the gray level of detected noisy pixel using Eq. (2). The proposed noise detection and removal process is also demonstrated by illustration 1 and illustration 2 using an example of 3×3 filtering window.

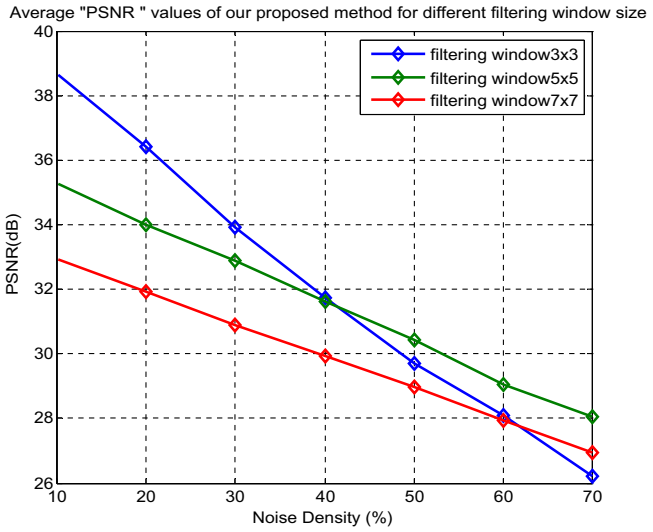

Fig. 4. Comparative graph of average performance of proposed method using different size of filtering window considering four test images of Fig. 2.

Illustration: Case1

STEP-1: A filtering window is selected

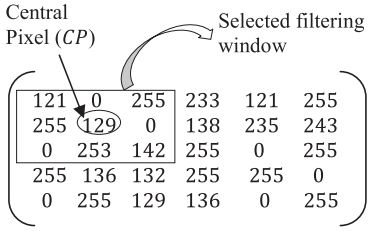

STEP-2: Now dual threshold values are computed for noise detection

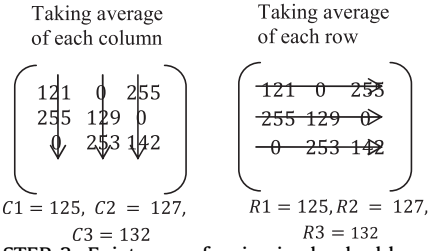

STEP-3: Existence of noise is checked by comparing the Central Pixel (CP) with thresholds

STEP-4: Since the CP value lies in between the two thresholds, the central pixel (CP) is considered to be noise free and remains unchanged

Illustration: Case2

STEP-1: A filtering window is selected

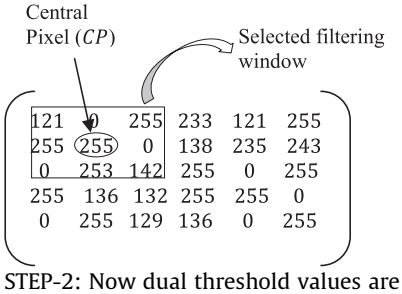

STEP-2: Now dual threshold values are computed for noise detection

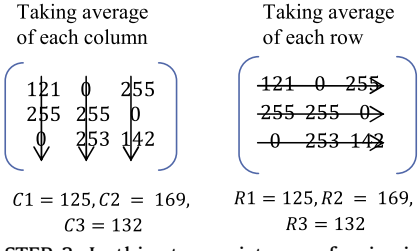

STEP-3: In this step, existence of noise is checked by comparing the CP with thresholds

STEP-4: Since the CP value is not lying in between the two thresholds, the central pixel (CP) is considered to be noisy

STEP-5: Since the CP is noisy, it will be replaced by median value of filtered window i.e. 142

5. Simulation and results

The simulations results have been drawn using MATLAB 7.5 on 2.5 GHz processor of 4 GB RAM. The results have been tested on gray scale JPEG images of size 256×256. The performance of proposed image de-noising method is analyzed on the basis of *Peak Signal to Noise Ratio* (PSNR). For the de-noised image "Z", of size $M \times N$, the PSNR [13] is given by:

$$\text{PSNR} = 10\log_{10}\frac{(255)^2}{\text{MSE}} \tag{12}$$

where MSE (Mean Square Error), is

$$\text{MSE} = \frac{\sum_{i=1}^{m}\sum_{j=1}^{n}\{Z(i,j) - A(i,j)\}^2}{M \times N} \tag{13}$$

where A is the noise-free (original) image.

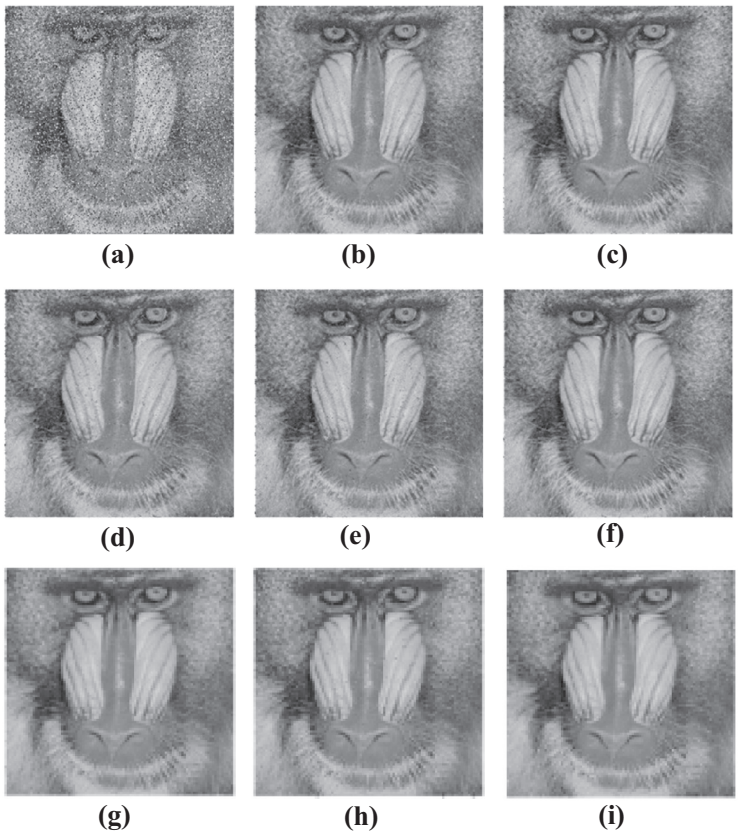

Fig. 5. Results of different filters in restoring 30% corrupted Mandrill image: (a) Noisy Image, (b) MED [1], (c) TSMF [7], (d) PSMF [12], (e) CWMF [9], (f) Luo [13], (g) ASWM [14], (h) ANSM [15] and (i) proposed method.

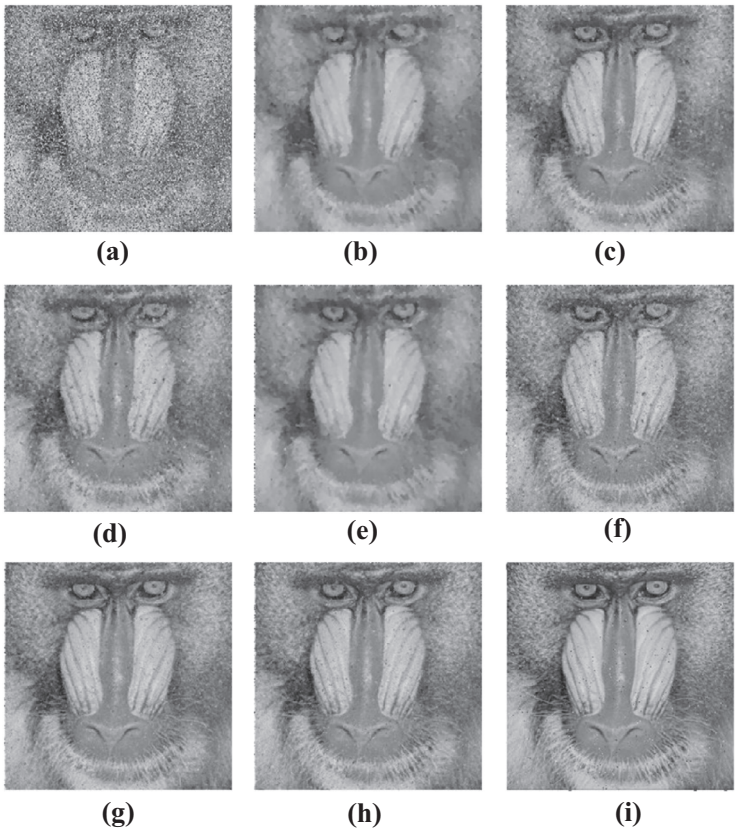

Fig. 6. Results of different filters in restoring 50% corrupted Mandrill image: (a) Noisy Image, (b) MED [1], (c) TSMF [7], (d) PSMF [12], (e) CWMF [9], (f) Luo [13], (g) ASWM [14], (h) ANSM [15] and (i) proposed method.

The simulations have been tested on the four standard images of Fig. 2. All of them are 8bpp images of size 256×256. The performance of proposed image denoising method is investigated for 10% to 70% noise density.

The quality performance of various image de-noising methods is illustrated in Table 1, when applied on Mandrill image, for RVIN density ranging from 10% to 70%. The PSNR value of de-noised image decreases with increase in percentage noise density for all the methods. As shown, proposed method reports much higher PSNR as compared to other denoising filters. It results 9.84% to 24.68% and 24.71% to 33.89% improvement in PSNR value as compared to ANSM method [15] and simple median filtering (MED) method respectively.

Results obtained with different de-noising methods for Goldhill image are represented in Table 2. Quality performance (PSNR) of proposed method reports 4.32% to 22.66% and 20.01% to 34.99% rise when judged with ANSM method [15] and MED method respectively. Interestingly, the rate of fall in PSNR of our proposed method is also less with respect to ANSM, ASWM, Lou's and TSM filters.

In Table 3, PSNR values obtained through different median filter based de-noising methods for Pepper image are shown. As compared to ANSM filtering based de-noising, proposed method results in an improvement of 2.09% to 12.99%.

For Lena image, results are given in Table 4. The PSNR outcome of proposed method is superior to all the other methods for noise densities up to 40%. Beyond 40% noise density, the performance becomes approximately equal to ASWM and ANSM filters. It offers 16.83–34.67% enhancement in quality when evaluated with respect to MED method.

The average performance of our proposed method, considering four test images corrupted by RVIN is represented in Table 5 and Fig. 3. The quality of de-noised image using our proposed method is improved to a greater extent. It reports 9.43% to 14% and 25.83% to 31.79% higher PSNR when judged with respect to ANSM method and MED method respectively. In Fig. 3, it is clearly visible that the performance curve of our proposed method is well above the existing de-noising methods.

Among the existing methods, ANSM method [15] produces best results. In order to check the statistical significance of proposed method with respect to ANSM method, the Mann–Whitney test is performed to verify the hypothesis statistically [23,24]. Firstly the test is conducted on five PSNR samples of both the methods for 60% noise density. It gives the rank total of 16 and 39 for ANSM and proposed method respectively. It results a "U" value equal to 1.

If $U \leqslant U_{critical}$, the hypothesis is considered as significant. In five sample test $U_{critical}$ is 2 for 5% level of significance (P-$value = 0.05$) [25]. Thus in this test proposed method proves its superiority over the ANSM method [15]. Secondly the test is repeated with 25 samples, considering PSNR obtained for all the noise densities ranging from 10% to 70% for both the methods. The test results a "U" value equal to 199 while the $U_{critical} = 211$ for $N1 = N2 = 25$ [26], hence proposed method can be well-thought-out to be significant. Along with this, the P-$value$ in the test is obtained as 0.02834 which is less than 0.05. It shows an edge over the ANSM method and a higher probability of occurrence of quoted results.

The effect of variation in the size of filtering window is represented in Table 6 and Fig. 4. As we can see PSNR of de-noised image in our proposed method decreases with increase in noise density for all the three window sizes. The decay in PSNR with increase in noise density is highest for $r = 3$ and decreases with increase in r. The average performance decreases from 35.25 dB to 28.06 dB for 5×5 filtering window as compared to 38.63 dB to 26.21 dB for 3×3 filtering window. This decay is still lesser for

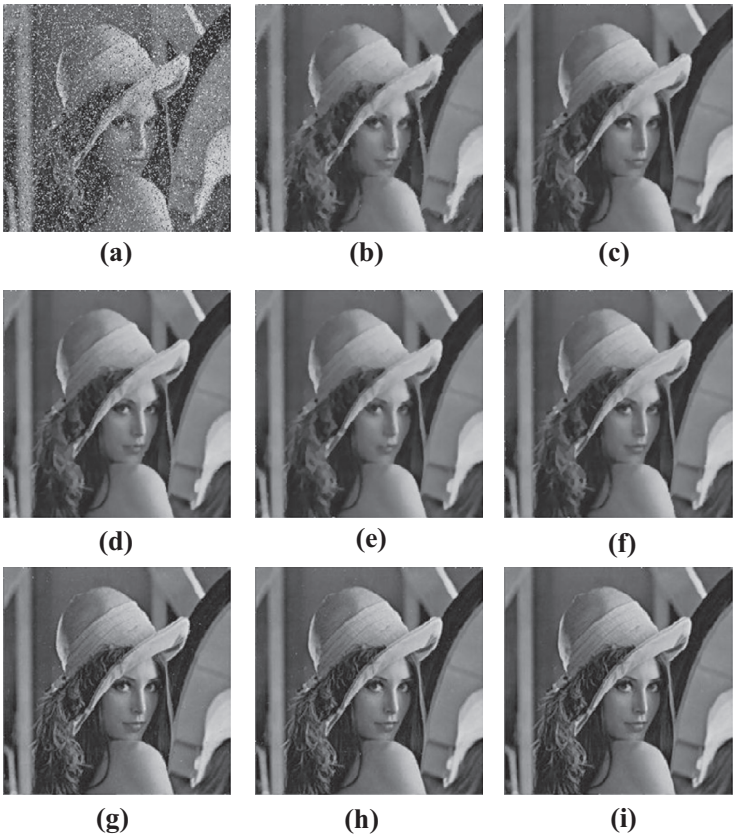

Fig. 7. Results of different filters in restoring 30% corrupted Lena image: (a) Noisy Image, (b) MED [1], (c) TSMF [7], (d) PSMF [12], (e) CWMF [9], (f) Luo [13], (g) ASWM [14], (h) ANSM [15] and (i) proposed method.

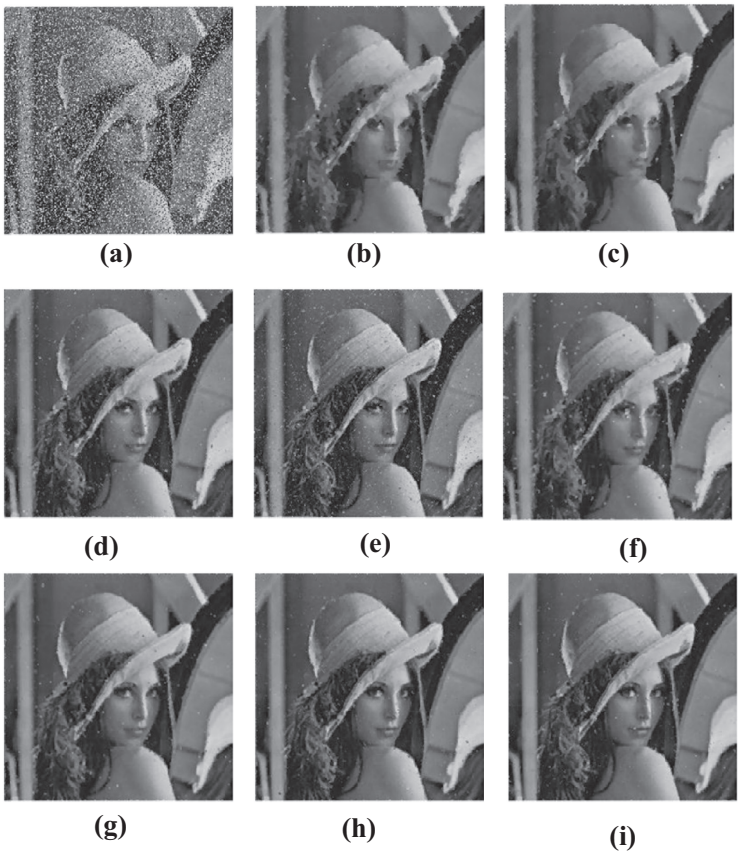

Fig. 8. Results of different filters in restoring 50% corrupted Lena image: (a) Noisy Image, (b) MED [1], (c) TSMF [7], (d) PSMF [12], (e) CWMF [9], (f) Luo [13], (g) ASWM [14], (h) ANSM [15] and (i) proposed method.

7x7 filtering window size i.e. from 32.92 dB to 26.95 dB. The PSNR of de-noised image with 3×3 window attains the highest level up to 40% noise density. By increasing this noise density further, the performance with 5×5 window size becomes better and improvised. The quality performance of image de-noising methods is image dependent. With increase in window size, number of pixels in any window increases which results in higher complexity and time consumption. For lower noise density, number of pixels corrupted by noise are less which results in high value of PSNR with smaller window size. For higher noise densities number of pixels corrupted by noise are significant hence the PSNR of de-noised image with higher window size attains greater value due to higher accuracy resulting from more number of pixels under consideration for detection of noise at any specific pixel. Due to all these reasons, estimation of optimum value of r is not feasible and no fixed rule may be defined for finding out the optimum value of r.

Image results of different filters on Mandrill image for 30% noise corruption by RVIN are given in Fig. 5. PSNR value of our proposed method is calculated as 32.77 dB, which is the best among all. Further in Fig. 6, the results of Mandrill image are given for 50% noise density. Proposed method provides the PSNR of 29.87 dB at this level, showing a reduction of 8.9% as compared to 30% noise corruption.

Figs. 7 and 8 show the results of different filters in restoring Lena image corrupted by 30% and 50% noise density respectively. The quality of restored image by the proposed method is the best, both qualitatively and quantitatively. The obtained PSNR of our proposed method is 34.67 dB and 29.15 dB at the noise level of 30% and 50% respectively.

6. Conclusion

This paper presents and explores an innovative approach of image de-noising with adaptive dual thresholds. The ideation and generation of the whole process is defined and illustrated in two stages i.e. Noise Detection and Noise Removal. In noise detection stage, the concept of averaging based dual threshold method is used which offers high noise detection ability and efficiency. Simple Median Filter is used for noise removal. Simulation results also show that the proposed dual threshold scheme is significantly superior to several state-of-the-art methods, both visually and quantitatively. The quality performance is image dependent and reports up to 24.92% and 22.66% higher PSNR when evaluated with ASWM and ANSM filters respectively at a noise level of 70%. It improvises vastly the de-noised image quality of Simple Median Filter from 16.38% to 33.89% for 70% noise density.

Acknowledgments

The authors would like to thank the faculty members of department of Electronics and Communication of MANIT, Bhopal (M.P.) India for their valuable suggestions and support at every step of the work.

References

[1] R.C. Gonzalez, R.E. Woods, Digital Image Processing, Prentice Hall, New Jersey, 2002.
[2] J. Astola, P. Kuosmaneen, Fundamentals of Nonlinear Digital Filtering, CRC, BocaRaton, FL, 1997.

[3] Ali S. Awad, Standard deviation for obtaining the optimal direction in the removal of impulse noise, IEEE Signal Process. Lett. 18 (7) (2011) 407–410.
[4] Ilke Turkmen, A new method to remove random-valued impulse noise in images, Int. J. Electron. Commun. (AEÜ) 67 (9) (2013) 771–779.
[5] Pinar. Civicioglu, Removal of random-valued impulsive noise from corrupted images, IEEE Trans. Consumer Electron. 55 (4) (2009) 2097–2104.
[6] Yu Hancheng, Li Zhao, Haixian Wang, An efficient procedure for removing random-valued impulse noise in images, IEEE Signal Process. Lett. 15 (2008) 922–925.
[7] T. Chen, K.-K. Ma, L.-H. Chen, Tri-state median filter for image denoising, IEEE Trans. Image Process. 8 (12) (1999) 1834–1838.
[8] A. Nieminen, P. Heinonen, Y. Neuvo, A new class of detail-preserving filters for image processing, IEEE Trans. Pattern Anal. Machine Intell. 9 (1) (1987) 74–90.
[9] S.-J. Ko, Y.H. Lee, Center weighted median filters and their applications to image enhancement, IEEE Trans. Circ. Syst. 38 (9) (1991) 984–993.
[10] E. Abreu, M. Lightstone, S.K. Mitra, K. Arakawa, A new efficient approach for the removal of impulse noise from highly corrupted images, IEEE Trans. Image Process. 5 (6) (1996) 1012–1025.
[11] E.J. Coyle, J.-H. Lin, M. Gabbouj, Optimal stack filtering and the estimation and structural approaches to image processing, IEEE Trans. Acoust. Speech Signal Process. 37 (12) (1989) 2037–2066.
[12] Z. Wang, D. Zhang, Progressive switching median filter for the removal of impulse noise from highly corrupted images, IEEE Trans. Circ. Syst. II: Analog Digital Signal Process. 46 (1) (1999) 78–80.
[13] W. Luo, A new efficient impulse detection algorithm for the removal of impulse noise, IEICE Trans. Fundam. Electron. Commun. Comput. Sci. E88 (10) (2005) 2579–2586.
[14] S. Akkoul, R. Lédée, R. Leconge, R. Harba, A new adaptive switching median filter, IEEE Signal Process. Lett. 17 (6) (2010) 587–590.
[15] Xia Lan, Zhiyong Zuo, Random-valued impulse noise removal by the adaptive switching median detectors and detail-preserving regularization, Optik – Int. J. Light Electron. Opt. 125 (3) (2014) 1101–1105.
[16] Dong Fuguo, Fan Hui, Yuan, A novel image median filtering algorithm based on incomplete quick sort algorithm, Int. J. Digital Content Technol. Appl. 4 (6) (2010) 79–83.
[17] K.S. Srinivasan, D. Ebenezer, A new fast and efficient decision-based algorithm for removal of high-density impulse noises, IEEE Signal Process. Lett. 14 (3) (2007) 189–192.
[18] Benzarti Faouzi, Hamid Amiri. Image denoising using non linear diffusion tensors. In: 8th IEEE international multi-conference on systems, signals & devices; 22–25 March 2011. p. 1–5.
[19] Ju Shen, Sen-Ching S. Cheung. Layer depth denoising and completion for structured-light RGB-D cameras. In: IEEE conference on computer vision and pattern recognition (CVPR); 23–28 June, 2013. p. 1187–94.
[20] Yuji Karita, Toshiyuki Tanaka. Restoration of original image from deteriorated image by probabilistic image model. In: SICE annual conference; August 20–22, 2008. p. 3096–100.
[21] Harold Christopher Burger, Bernhard Scholkopf, Stefan Harmeling. Removing noise from astronomical images using a pixel-specific noise model. In: IEEE international conference on computational photography (ICCP); 8–10 April, 2011. p. 1–8.
[22] Johannes R. Sveinsson, Jon Atli Benediktsson. Speckle reduction of SAR images using wavelet-domain hidden Markov models. In: Proceedings of IEEE international geosciences and remote sensing symposium (IGARSS 2000) 4; 24–28 July 2000. p. 1666–8.
[23] L.C. Dinneen, B.C. Blakesley, AS 62, a generator for the sampling distribution of the Mann-Whitney U statistic, Appl. Stat. 22 (2) (1973).
[24] E.F. Harding, An efficient minimal storage procedure for calculating the Mann-Whitney U, generalised U and similar distributions, Appl. Stat. (1983) 33.
[25] http://www.sussex.ac.uk/Users/grahamh/RM1web/MannWhitneyHandout%202011.pdf.
[26] http://www.saburchill.com/IBbiology/downloads/002.pdf.